Neuroticism and the brain

Servaas, Michelle

8 Chapter

The triadic interplay between 5-HTTLPR/COMT, functional brain network organization and neuroticism

Michelle N. Servaas
Linda Geerligs
Jojanneke A. Bastiaansen
Remco J. Renken
Jan-Bernard C. Marsman
Ilja M. Nolte
Johan Ormel
André Aleman
Harriëtte Riese

Under review

8.1 Abstract

Neuroticism and genetic variation in the serotonin-transporter (SLC6A4) and catechol-O-methyltransferase (COMT) gene are risk factors for psychopathology. Studies have proposed that these vulnerabilities are associated with alterations in the functional integration and segregation of neural circuits. The aim of the current study was to investigate the triadic interplay between genetic variation in the SLC6A4 and COMT gene, functional brain network organization and neuroticism. We applied graph theory analysis on resting-state fMRI data in a sample of 120 women selected based on their neuroticism score and genotyped two polymorphisms: 5-HTTLPR and COMT (rs4680-rs165599). In genetic risk carriers compared to non-risk carriers, we observed that subnetworks related to salience and visual processing play a more prominent role in the functional network organization than subnetworks related to cognitive control. COMT (not 5-HTTLPR) moderated the association between neuroticism and functional network organization. In the genetic risk group (not the non-risk group), neuroticism was associated with lower efficiency coefficients in salience and sensory(-motor) subnetworks and higher participation coefficients in the fronto-parietal control subnetwork. To conclude, the findings of altered topology of specific subnetworks may help explain why risk carriers of 5-HTTLPR and COMT (scoring higher on neuroticism) are more prone to develop psychiatric disorders.

8.2 Introduction

Neuroticism is a robust personality trait that is part of various widely accepted personality theories and models (Costa and McCrae, 1992; Eysenck, 1967; Gray, 1991) and can be defined as the tendency to react with a negative emotional response to life experiences (Ormel et al., 2013a). It has been well established as a potent risk marker for a range of psychiatric disorders, particularly internalizing disorders (Lahey, 2009; Ormel et al., 2013b). Furthermore, high compared to low neurotic individuals have more comorbid disorders, unexplained medical issues and general health problems (Lahey, 2009). In addition, besides being a heavy burden on the individual, high neuroticism is also an important burden for society as its economic costs exceed those of common mental disorders, such as affective disorders and substance-related disorders (Cuijpers et al., 2010).

It is evident that neuroticism is a relevant concept for public health and that it is important to unravel its genetic basis and underlying neurobiological mechanisms. Prior research has indicated that neuroticism is moderately heritable, that is, approximately half of the variance can be explained by genetic factors (Boomsma et al., 2000; Distel et al., 2009; Hansell et al., 2012; Riese et al., 2009). Two genes that have been associated with neuroticism and emotion processing are the serotonin transporter (SLC6A4) gene and catechol-O-methyltransferase (COMT) gene (for reviews, see Bevilacqua and Goldman, 2011; Canli, 2008; Domschke and Dannlowski, 2010; Hariri and Holmes, 2006). First, the SLC6A4 gene is an important regulator of serotonergic neurotransmission through the reuptake of serotonin (5-hydroxtryptamine, 5HT) from the synaptic cleft in, among others, limbic regions of the brain (Bevilacqua and Goldman, 2011; Hariri and Holmes, 2006). A common length polymorphism (5-HTTLPR) is located in the promotor region of this gene and encodes two alleles: a short (S) allele and a long (L) allele (Bevilacqua and Goldman, 2011; Hariri and Holmes, 2006). Carrying the S-allele has been associated with lower serotonin transporter binding and mRNA expression as well as lower serotonin uptake compared to carrying two copies of the L-allele (Lesch et al., 1996). Furthermore, the L-allele is functionally regulated by an A to G substitution in the single-nucleotide polymorphism (SNP) rs25531 located close to 5-HTTLPR, making its transcriptional efficacy more comparable to the low-expressing S-allele (risk haplotypes include SS, SLg, SLa and LgLa) (Hu et al., 2006; Wendland et al., 2006).

Second, the COMT gene produces the enzyme COMT that inactivates catecholamine neurotransmitters dopamine, epinephrine and norepinephrine, specifically in the prefrontal cortex (PFC) (Mier et al., 2010). Enzyme function is in part influenced by a G to A substitution at codon 158 (rs4680), producing an amino acid change from valine (Val) to methione (Met) (Lachman et al., 1996). The Met-allele is thermolabile at normal body temperature and has a three-to-four fold reduction in enzyme activity compared to the Val-allele, leading to higher dopamine concentrations and more efficient information processing in the PFC (Chen et al., 2004; Egan et al., 2001; Lachman et al., 1996). Furthermore, a COMT haplotype containing the abovementioned SNP rs4680 and additional SNP rs165599 has been associated with neuroticism (risk haplotype:

GG-AA) (Hettema et al., 2008), potentially resulting in lower levels of cortical dopamine (Bray et al., 2003).

As is the case with many common mental disorders, neuroticism is polygenic in nature, that is, multiple mutations of small effect are involved in its development (Canli, 2008; Flint, 2004). For this reason, traditional association studies have regularly failed to find a link between such phenotypes and risk polymorphisms (Cannon and Keller, 2006). To overcome this problem, an approach was adopted that involves studying endophenotypes, which are intermediate phenotypes that lie in between the genotype and phenotype (Gottesman and Gould, 2003). The assumption is made that endophenotypes are more elementary in nature and because of that, implicate fewer genetic, environmental and epigenetic factors as well as interactions between them in producing phenotypic variation (Gottesman and Gould, 2003). Since neuroticism has been related to alterations in brain functioning (Servaas et al., 2013b), neural measures are ideal to be used as endophenotypes in the search for risk polymorphisms (i.e. imaging genetics) (Fornito and Bullmore, 2012; Tost et al., 2012). Recently, it has been proposed that psychopathology probably does not arise from dysfunctional activation in a few specific brain regions during a particular task, but from alterations in the functional integration and segregation of neural circuits (i.e. disrupted connectivity) (Buckholtz and Meyer-Lindenberg, 2012; Fornito et al., 2011; Fornito and Bullmore, 2012; Meyer-Lindenberg, 2012; Tost et al., 2012).

In our previous paper of this sample, we investigated alterations in the functional network organization associated with neuroticism using graph theory (i.e. imaging connectomics) (Servaas et al., 2014b). In short, we found that the functional network structure of high compared to low neurotic individuals is organized less optimally with regard to efficient information processing and shows signs of functional disconnectivity. Furthermore, we demonstrated that subnetworks related to emotion and salience processing play a more prominent role in the network organization of high neurotic individuals, while subnetworks related to sensory(-motor) functions and cognitive control play a less prominent role.

The aim of the current study was to investigate the triadic interplay between genetic variation in the SLC6A4 and COMT gene, functional brain network organization and neuroticism, since these factors may be part of a pathway from genotype to phenotype. To this end, we applied graph theory analysis on resting-state functional magnetic resonance imaging (rs-fMRI) data in a sample of 120 women selected on the basis of their neuroticism score and genotyped two polymorphisms: 5-HTTLPR and COMT (rs4680-rs165599). For both polymorphisms, we hypothesized to find an altered functional network organization in genetic risk carriers compared to non-risk carriers (see method section for the group definition). Specifically, we hypothesized that subnetworks related to emotion and salience processing play a more prominent role in the functional network organization of these genetic risk carriers, than subnetworks related to cognitive control. Additionally, we assessed the abovementioned triadic interplay with an interaction analysis, wherein we tested the

moderation effect of 5-HTTLPR/COMT (rs4680-rs165599) on the association between functional network organization and neuroticism. This is in line with former genetic imaging studies on traits (Drabant et al., 2006; Hahn et al., 2011, 2013; Shehzad et al., 2012). As a potential underlying biological mechanism, Hahn et al. (2011, 2013) speculated that polymorphisms may influence neural (network) plasticity (in interaction with the (early) environment) via neurotransmission during development.

8.3 Methods and materials

8.3.1 Participants

Initially, 240 students from the University of Groningen were asked to fill out the NEO Five-Factor Inventory (NEO-FFI) (domains Neuroticism and Extraversion, 24 items). Individuals were sent a questionnaire when they agreed to participate in the study (based on the information letter, which included an informed consent form) and met the following selection criteria: 1) female gender, 2) age between 18-25 years, 3) Dutch as native language, 4) Caucasian descent, 5) right handed, 6) no use of contraceptive medication, except for oral contraceptive pills (21-pill packet). Only females were included because they significantly score higher on neuroticism than men and because of that, have a higher risk of developing affective disorders (Parker and Brotchie, 2010). Furthermore, research is still limited related to gender differences in neuroticism, therefore, we decided not to introduce this variation in the sample as it is not properly understood yet. Exclusion criteria were 1) a history of seizure or head injury, 2) a life time diagnosis of psychiatric and/or neurological disorders, 3) a life time diagnosis of psychiatric disorders in first degree relatives of the participant, 4) the use of medication that can influence test results, 5) visual or auditory problems that cannot be corrected, 6) MRI incompatible implants or tattoos, 7) claustrophobia, 8) suspected or confirmed pregnancy. From this sample, 120 individuals (mean age: 20.8 SD ± 2.0, age range: 18-25) were invited to participate in the experiment. To ensure sufficient numbers of participants with high levels of neuroticism, sixty individuals were selected from the highest quartile of neuroticism scores (NEO-FFI score ≥ 32, range 32-47) and sixty individuals were randomly selected from the three lowest quartiles (NEO-FFI < 32, range 17-31). Plots of normality (QQ-plot and boxplot) showed that, in the selected 120 participants, neuroticism scores were approximately normally distributed.

In order to reduce hormone-related between-subject variability, participants were invited for the experiment during the first ten days of their menstrual cycle (early and mid-follicular phase) or during the discontinuation week in case of oral contraceptive usage, which resembles the early and mid-follicular phase in terms of ovarian hormonal levels (Cohen and Katz, 1979). During these phases, ovarian hormonal levels are relatively low and menstrual cycle related changes in mood, stress sensitivity and neurocognitive function are minimal (Andreano and Cahill, 2010; Goldstein et al., 2010; Symonds et al., 2004).

On the day of the experiment, after explaining the procedure, participants gave informed consent for a second time and completed the NEO Personality Inventory Revised (NEO-PI-R) (domains Neuroticism, Extraversion and Conscientiousness, 144 items) (Hoekstra et al., 1996). In addition, the study was approved by the Medical Ethical Committee of the University Medical Center Groningen and was conducted in accordance with the Declaration of Helsinki.

8.3.2 Genotyping

DNA extraction and genotyping were performed at the department of Laboratory Medicine of the University Medical Center Groningen, Groningen, the Netherlands. Saliva was collected in Oragene saliva collection and preservation kits (DNAGenotek, Ontario, Canada), and DNA was extracted according to the protocol of the manufacturer.

For the SLC6A4, the 5-HTTLPR S/La/Lg variants were determined using PCR with Forward primer FAM-5'TGAATGCCAGCACCTAACCC-3' and Reverse primer 5-TTCTGGTGCCACCTAGACGC-3' (35 cycli of 30 seconds at 95°C, 30 seconds at 61°C and 1 minute at 72°C), and subsequent ingestion of the PCR product with the restriction enzyme Msp-I for at least 3 hours at 37 °C. The resulting restriction fragments were separated using capillary electrophoresis (ABI 3130 analyzer; Applied Biosystems, Nieuwerkerk a/d IJssel, the Netherlands), and fragment lengths were estimated using the ABI Prism® GeneMapper™ software, version 3.0 (Applied Biosystems). The La, Lg and S variants were determined by the detection of fragments of 325 base pairs (bp), 152 bp and 284 bp, respectively (validated in-house method, Doornbos et al., 2009). In the remainder of this paper, the Lg allele will be referred to as the S allele and the La allele as the L allele (Wendland et al., 2006).

Genotyping of the COMT rs4680 polymorphism (1947 G/A; Val_{158}Met; GenBank Z26491) was performed with the allelic discrimination technique following the protocol supplied by Applied Biosystems. We used primers COMT-GAF (5'-CGAGATCAACCCCGACTGT-3') and COMT-GAR (5'-CAGGCATGCACACCTTGTC-3'), and minor grove-binding probes VIC-5'-TTTCGCTGGCGTGAAG-3'-NFQ (G) and FAM-5'-TCGCTGGCATGAAG-3'-NFQ (A). COMT rs165599 was genotyped using the commercially available kit C_2255335_10 (Applied Biosystems). All COMT reactions were carried out in TaqMan universal PCR master mix using a 7500 Real-Time PCR System (Applied Biosystems).

8.3.3 Genotype analysis

We used PHASE (v2.1.1) (Stephens et al., 2001) to reconstruct two-marker haplotypes from the COMT SNPs rs4680 and rs165599. For each subject, haplotype frequencies were determined and used to estimate the genotype probabilities of haplotype pairs. When a genotype probability exceeded 0.80, the corresponding haplotype pair was assigned. However, when all genotype probabilities were smaller than 0.80, haplotypes were set to missing. In the current study, all

genotype probabilities exceeded 0.80. In the remainder of this paper, the haplotype COMT rs4680-rs165599 will be referred as COMT.

Subjects were grouped into genetic risk carriers and non-risk carriers for the two polymorphisms (Hettema et al., 2008; Hu et al., 2006; Wendland et al., 2006). For 5-HTTLPR, risk genotypes include S/S and S/L and the non-risk genotype includes L/L (Wendland et al., 2006). For COMT, risk haplotypes include Val/Val for rs4680 and Met/Met for rs165599 and non-risk haplotypes include Met/Met and Val/Met for rs4680 and Val/Val en Val/Met for rs165599 (Hettema et al., 2008).

Hardy-Weinberg equilibrium was tested for 5-HTTLPR, COMT rs4680 and COMT rs165599 using a chi-square test with one degree of freedom.

8.3.4 Image acquisition

A 3 Tesla Philips Intera MRI scanner (Philips Medical Systems, Best, the Netherlands), equipped with a 32-channel SENSE head coil, was used to acquire the images. A high-resolution T1-weighted 3D structural image was obtained using fast-field echo (FFE) for anatomical reference (170 slices; TR: 9 ms; TE: 8 ms; FOV: 256 x 231; 256 x 256 matrix; voxel size: 1 x 1 x 1 mm). rs-fMRI images were acquired with a T2*-weighted gradient echo planar imaging (EPI) sequence. Participants were instructed to close their eyes and to not fall asleep. The scan comprised 300 volumes of 37 axial-slices (TR: 2000 ms; TE: 30 ms; FOV: 220 x 221; 64 x 62 matrix; voxel size: 3.5 x 3.5 x 3.5 mm). Slices were acquired in descending order without a gap. To prevent artifacts due to nasal cavities, images were tilted 10° to the AC-PC transverse plane (see Supplemental material S1 for more details on the full fMRI session).

8.3.5 Data preprocessing

Image processing was performed using SPM8 (http://www.fil.ion.ucl.ac.uk/spm), implemented in Matlab 7.8.0 (The Mathworks Inc., Natick, MA). Preprocessing included realignment, coregistration, DARTEL normalization (2 x 2 x 2 mm isotropic voxels) (Ashburner, 2007) and smoothing (8 mm full-width at half maximum (FWHM) Gaussian kernel) (see Supplemental material S2 for details on the preprocessing steps).

Next, a series of preprocessing steps specific to rs-fMRI analysis were performed. First, regression of several nuisance variables was applied per grey matter voxel to remove sources of spurious variance, comprising six rigid body head motion parameters, the global signal, white matter (WM) signal and cerebrospinal fluid (CSF) signal. In order to obtain the last two signals, we performed segmentation of the T1-weighted image to create a WM and CSF mask and extracted the first eigenvariate from the time series of the included voxels. In addition, the first temporal derivatives of abovementioned nuisance variables were removed. Second, temporal band-pass

filtering was applied to detrend the signal and to retain frequencies between 0.008-0.08Hz (Van Dijk et al., 2010). Third, we performed scrubbing to additionally remove influences of movement on the rs-fMRI data (Power et al., 2012) (see Supplemental material S3 for details on the scrubbing procedure).

After data preprocessing, nine participants were excluded from further analysis; two because of anatomical abnormalities (i.e. large ventricles that were still within the normal range, but difficult to normalize), five because of technical difficulties and two because of excessive scrubbing (more than one-third of the volumes had to be removed). Furthermore, for COMT, two additional subjects had to be excluded due to failure of genotyping. The following total samples remained for statistical analysis: for 5-HTTLPR, a sample of 111 participants and for COMT, a sample of 109 participants.

8.3.6 Network construction

In order to perform graph theory analysis, nodes and edges have to be defined. For nodes, a sphere of 5 mm radius was created around 264 coordinates provided by Power et al. (2011). After visual inspection of the regions of interest (ROIs), we noted the absence of three relevant subcortical structures for research on neuroticism: bilateral amygdala, hippocampus and caudate (Servaas et al., 2013b). The coordinates for these regions were determined using the Harvard-Oxford Subcortical Structural Atlas (80% probability), resulting in a total of 270 ROIs. No overlap was observed between the additional ROIs and the ROIs of Power et al. (2011). Next, we binarized the functional images of all subjects and built a whole-brain group mask by multiplying them. This locates the parts of the brain, where EPI images were free from susceptibility artifacts in all subjects. Subsequently, the overlap was calculated voxel-wise between all ROIs and the group mask. When a ROI overlapped <50% with the group mask, it was excluded from further analysis. This was the case for eleven ROIs. To construct a connectivity matrix per subject, we extracted the regional mean time series for each of the remaining 259 ROIs and calculated Pearson correlations between all pairs. Furthermore, to prevent biases due to shared non-biological signals between adjacent ROIs, correlations were set to zero when the distance was less than 20 mm between the centres of two ROIs (Power et al., 2011). In addition, correlations on the diagonal of the connectivity matrix were set to zero as well.

8.3.7 Thresholding

It has been shown that the majority of network measures are highly sensitive to the number of edges in a graph (van Wijk et al., 2010). To avoid this confound, we applied a range of proportional thresholds to each correlation matrix per subject. The threshold values (T) ranged from 0.01 to 0.30 in increments of 0.01. Network measures were calculated on the whole-brain and different functional subnetworks for both binary and weighted graphs across the selected

range of threshold values (see below). In order to partition the graph into modules, we applied the algorithm of Blondel et al. (2008) and the modularity fine-tuning algorithm of Sun et al. (2009) (see Supplemental material S4 for details on the module decomposition). For this procedure, we selected a single optimal threshold by applying the method described in Geerligs et al. (2014). The optimal threshold in the current study was 1.8% (see Supplemental material S5 for details on the selection of the optimal threshold).

8.3.8 Network modules

In our previous paper (Servaas et al., 2014b), we found that nodes could be partitioned in six functional subnetworks with a maximum number of within-group edges and a minimum number of between-group edges (Rubinov and Sporns, 2010) (see Supplemental material S4 for details on the module decomposition). These included the affective subnetwork (AS), cingulo-operculum subnetwork (COS), default mode subnetwork (DMS), fronto-parietal subnetwork (FPS), somatosensory-motor subnetwork (SMS) and visual subnetwork (VS) (for figures of the module decomposition, see Figure 2 and 3 in Servaas et al., 2014b). This modular decomposition was used in subsequent analyses.

8.3.9 Network measures

Network measures were calculated on binary as well as weighted graphs across the selected range of threshold values by using functions implemented in the Brain Connectivity Toolbox (www.brain-connectivity-toolbox.net, Rubinov and Sporns, 2010). In binary networks, an edge is indicated as present or not, providing information on the functional network structure. In weighted networks, edge strengths are preserved, additionally providing information on the functional connectivity strength (Rubinov and Sporns, 2010). First, we calculated the whole-brain network measures: global efficiency (E_{global}), local efficiency (E_{local}, averaged across nodes) and maximized modularity (Q). Global efficiency is calculated as the average inverse shortest path length between all pairs of nodes. Local efficiency is calculated in a similar manner, but then between a node and its direct neighbours (Latora and Marchiori, 2001; Rubinov and Sporns, 2010). Maximized modularity is calculated with a function that quantifies the degree to which a network can be clearly delineated in non-overlapping groups of nodes (Newman, 2004; Rubinov and Sporns, 2010). Second, we calculated local efficiency (E_{local}, averaged across nodes) and the participation coefficient (Y, averaged across nodes) per module. The participation coefficient is calculated as the ratio of intra- versus intermodular connections per node (Rubinov and Sporns, 2010).

8.3.10 Network analyses

Across the selected range of threshold values, we calculated i) the mean difference between the genetic risk and non-risk group per network measure for each polymorphism, ii) the difference

in slope between the genetic risk and non-risk group for the association between neuroticism and a specific network measure for each polymorphism. These difference measures were plotted and visually checked for consistency across threshold values. Subsequently, we applied the threshold-free cluster enhancement (TFCE) method per network measure across threshold values to obtain a summarized scalar that is independent of single threshold selection (settings: E=1, H=0, hmin=0, hmax=maximal difference, dh=1000) (Smith and Nichols, 2009). Next, non-parametric permutation testing was applied on the TFCE per network measure to assess whether the results could have occurred by chance. To this end, genetic group membership was permuted randomly and both difference measures were recalculated per network measure for each polymorphism. This procedure was repeated 5000 times and a one-tailed test of the null hypothesis ($p<0.05$) was performed (Zhang et al., 2011).

8.4 Results

8.4.1 Sample characteristics

The mean NEO-PI-R neuroticism score across the whole sample was 135.5 SD ± 18.9 (range: 94-195). The genotype and allele frequencies closely resembled findings from the European HapMap31 (5-HTTLPR, L/L = 31, L/S = 57, S/S = 32, L = 0.50, S = 0.50; COMT rs4680, A/A = 34, A/G = 57, G/G = 28, A = 0.53, G = 0.47; COMT rs165599, A/A = 56, A/G = 51, G/G = 11, A = 0.69, G = 0.31). The genotype distributions were in Hardy-Weinberg equilibrium (5-HTTLPR, p = 0.58; COMT rs4680, p = 0.67; COMT rs165599, p = 0.90). For 5-HTTLPR, the risk genotype group comprised 80 individuals and the non-risk genotype group comprised 31 individuals. For COMT, the risk haplotype group comprised 42 individuals and the non-risk haplotype group comprised 67 individuals. For both polymorphisms, the risk group did not significantly differ from the non-risk group based on their mean neuroticism scores (5-HTTLPR $t_{(109)} = -0.72$, p = 0.48; COMT $t_{(107)} = -0.07$, p = 0.95).

8.4.2 Whole-brain network measures

8.4.2.1 Main effect of genetic group

For 5-HTTLPR, decreased global efficiency and increased modularity were found in the risk genotype group compared with the non-risk genotype group for binary graphs. For weighted graphs, we observed increased global efficiency, local efficiency and modularity in the risk genotype group contrasted with the non-risk genotype group. For COMT, we found decreased local efficiency and modularity in the risk haplotype group compared with the non-risk haplotype group for binary graphs. For weighted graphs, no significant results were identified (see Table 1 for the results).

8.4.2.2 Interaction effect between genetic group and neuroticism

COMT moderated the association between neuroticism and global efficiency for binary graphs. Specifically, neuroticism was positively correlated with global efficiency in the risk haplotype group, while a weak correlation was observed in the non-risk haplotype group. For weighted graphs, COMT moderated the association between neuroticism and local efficiency. Specifically, neuroticism correlated negatively with local efficiency in the risk haplotype group, while a weak correlation was found in the non-risk haplotype group (see Table 2 and Figure 1 for the results and see Supplemental material S6, Table S1 for the correlation values). No significant results were identified for 5-HTTLPR.

8.4.3 Network measures per module

8.4.3.1 Main effect of genetic group per module

For 5-HTTLPR, we found a decreased participation coefficient in the DMS, FPS and VS in the risk genotype group compared with the non-risk genotype group for both binary and weighted graphs. Additionally, we observed increased local efficiency in the COS and VS in the risk genotype group contrasted with the non-risk genotype group for weighted graphs. For COMT, we found decreased local efficiency in the DMS in the risk haplotype group compared with the non-risk haplotype group for binary graphs. For weighted graphs, a decreased participation coefficient in the FPS was observed in the risk haplotype group contrasted with the non-risk haplotype group (see Table 1 for the results).

8.4.3.2 Interaction effect between genetic group and neuroticism per module

For binary graphs, COMT moderated the association between neuroticism and local efficiency in the VS and between neuroticism and the participation coefficient in the FPS. For local efficiency in the VS, a negative correlation was observed with neuroticism in both genetic groups, however, this effect was more pronounced in the risk haplotype group. For the participation coefficient in the FPS, a positive correlation was found with neuroticism in the risk haplotype group, while a weak correlation was found in the non-risk haplotype group. For weighted graphs, COMT moderated the association between neuroticism and local efficiency in the COS, SMS and VS. In these three subnetworks, neuroticism was negatively correlated with local efficiency in the risk haplotype group, while a weak correlation was observed in the non-risk haplotype group (see Table 2 and Figure 1 for the results and see Supplemental material S6, Table S1 for the correlation values). For 5-HTTLPR, no significant results were identified.

Table 1 Results for the main effect of genetic group

Polymorphism	Graph type	Network measure	Global/ subnetwork	TFCE p-value	Contrast
COMT	Binary	Local efficiency	Global	0.05	risk < non-risk
COMT	Binary	Modularity	Global	0.02	risk < non-risk
COMT	Binary	Local efficiency	DMS	0.009	risk < non-risk
COMT	Weighted	Participation coefficient	FPS	0.044	risk < non-risk
5-HTTLPR	Binary	Global efficiency	Global	0.036	risk < non-risk
5-HTTLPR	Binary	Modularity	Global	0.034	risk > non-risk
5-HTTLPR	Binary	Participation coefficient	DMS	0.008	risk < non-risk
5-HTTLPR	Binary	Participation coefficient	FPS	0.003	risk < non-risk
5-HTTLPR	Binary	Participation coefficient	VS	0.027	risk < non-risk
5-HTTLPR	Weighted	Global efficiency	Global	0.041	risk > non-risk
5-HTTLPR	Weighted	Local efficiency	Global	0.033	risk > non-risk
5-HTTLPR	Weighted	Modularity	Global	0.035	risk > non-risk
5-HTTLPR	Weighted	Local efficiency	COS	0.039	risk > non-risk
5-HTTLPR	Weighted	Local efficiency	VS	0.023	risk > non-risk
5-HTTLPR	Weighted	Participation coefficient	DMS	0.008	risk < non-risk
5-HTTLPR	Weighted	Participation coefficient	FPS	0.001	risk < non-risk
5-HTTLPR	Weighted	Participation coefficient	VS	0.01	risk < non-risk

The measures global efficiency, local efficiency, modularity and participation coefficient were calculated on the whole-brain network and/or different functional subnetworks for binary and weighted graphs. The mean difference between the genetic risk and non-risk group was caluclated per network measure for each polymorphism. In the fifth column, p-values are listed for a one-tailed test of the null hypothesis ($p<0.05$) wherein we assessed whether the observed area under the curve could have occurred by chance using the threshold-free cluster enhancement (TFCE) method. COS, cingulo-operculum subnetwork; DMS, default mode subnetwork; FPS, fronto-parietal subnetwork; VS, visual subnetwork.

Table 2 Results for the interaction effect between COMT haplotype and neuroticism

Polymorphism	Graph type	Network measure	Global/ subnetwork	TFCE p-value	Contrast
COMT	Binary	Global efficiency	Global	0.036	risk > non-risk
COMT	Binary	Local efficiency	VS	0.023	risk < non-risk
COMT	Binary	Participation coefficient	FPS	0.042	risk > non-risk
COMT	Weighted	Local efficiency	Global	0.033	risk < non-risk
COMT	Weighted	Local efficiency	COS	0.045	risk < non-risk
COMT	Weighted	Local efficiency	SMS	0.026	risk < non-risk
COMT	Weighted	Local efficiency	VS	0.013	risk < non-risk

The measures global efficiency, local efficiency, modularity and participation coefficient were calculated on the whole-brain network and/or different functional subnetworks for binary and weighted graphs. The difference in slope between the genetic risk and non-risk group was calculated for the association between neuroticism and a specific network measure for each polymorphism In the fifth column, p-values are summed for a one-tailed test of the null hypothesis ($p<0.05$) wherein we assessed whether the observed area under the curve could have occurred by chance using the threshold-free cluster enhancement (TFCE) method. COS, cingulo-operculum subnetwork; FPS, fronto-parietal subnetwork; SMS, somatosensory-motor subnetwork; VS, visual subnetwork.

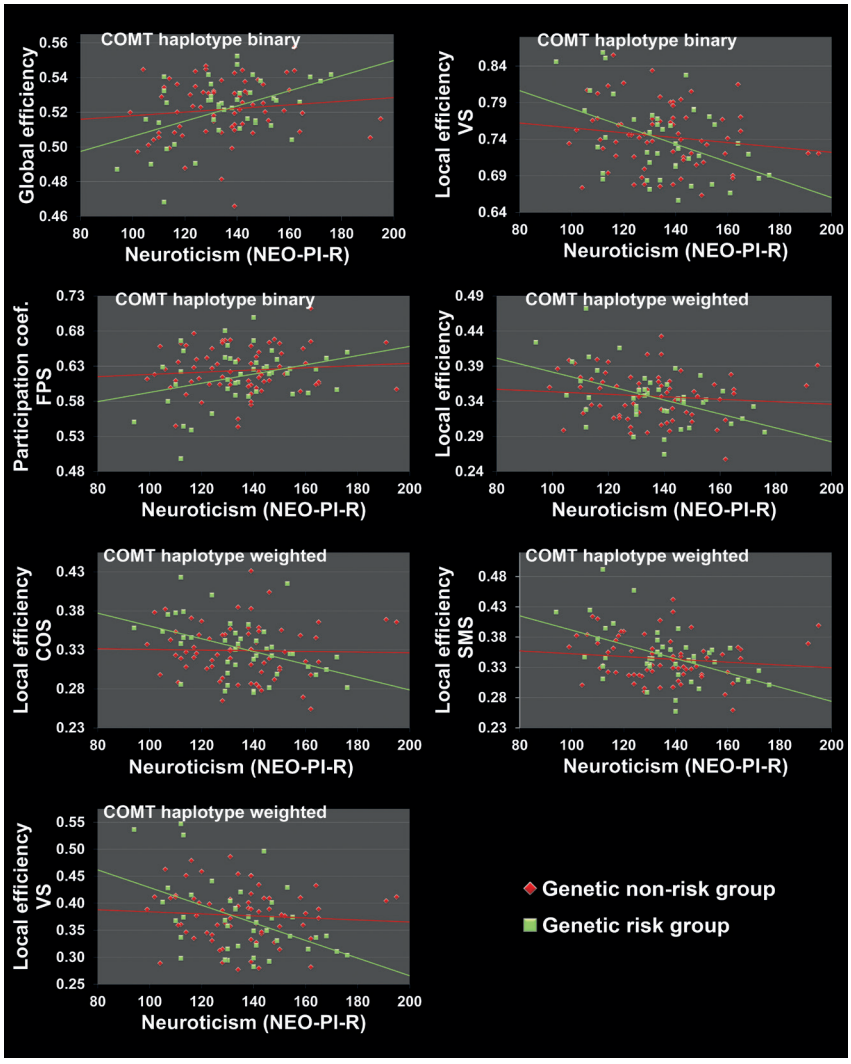

Figure 1 Results for the interaction effect between COMT haplotype and neuroticism. The measures global efficiency, local efficiency, modularity and participation coefficient were calculated on the whole-brain network and/or different functional subnetworks for binary and weighted graphs. The difference in slope between the genetic risk and non-risk group was calculated for the association between neuroticism and a specific network measure for each polymorphism (see the method section for the group definition). Results are visualized for the proportional threshold of 15%. Coef., coefficient; COMT, catechol-O-methyltransferase, COS, cingulo-operculum subnetwork; FPS, fronto-parietal subnetwork; NEO-PI-R, NEO personality inventory revised; SMS, somatosensory-motor subnetwork; VS, visual subnetwork.

8.5 Discussion

The aim of the current study was to investigate the triadic interplay between 5-HTTLPR/COMT, functional brain network organization and neuroticism. Consistent with prior hypotheses, we found an altered functional network organization in genetic risk carriers compared to non-risk carriers for both polymorphisms. Specifically, the findings showed a stronger involvement of subnetworks related to salience and visual processing in the functional network organization of genetic risk carriers and less involvement of subnetworks related to cognitive control. Moreover, COMT (but not 5-HTTLPR) moderated the association between neuroticism and functional network organization. In the risk haplotype group, individuals scoring higher on neuroticism (compared to individuals scoring lower) had lower efficiency coefficients for salience and sensory(-motor) subnetworks, while showing relatively more connections between the fronto-parietal control subnetwork and other functional subnetworks. This effect was not observed in the non-risk haplotype group.

8.5.1 5-HTTLPR

For 5-HTTLPR, in risk genotype carriers compared to non-risk genotype carriers, we found that the whole-brain functional network organization resembles more that of a small-world organization, that is, increased functional integration and segregation (Latora and Marchiori, 2001; for a description of the different types of network organizations, see Watts and Strogatz, 1998 and Xia and He, 2011). Specifically, we observed that efficiency coefficients were higher in salience and visual subnetworks (COS and VS) and that cognitive control and visual subnetworks (DMS, FPS and VS) had relatively fewer connections with other functional subnetworks. The salience subnetwork (COS) is involved in the detection and evaluation of salient affective stimuli and the production of affective states (Laird et al., 2011; Menon and Uddin, 2010; Seeley et al., 2007). It includes, among others, the insula, anterior cingulate cortex (ACC), striatum and thalamus. This subnetwork is important in identifying stimuli that pose a threat to survival and subsequently, launching a cascade of reactions that include the initiation of physiological and behavioural preparatory mechanisms for an adaptive response (Menon and Uddin, 2010; Seeley et al., 2007). During such threatening situations, sensory systems are modulated and tuned by neural circuitry via neurotransmitters in order to focus attention selectively on the salient stimulus (Hurley et al., 2004). Previous research has shown that the neurotransmitter serotonin can alter the responsivity and selectivity of sensory neurons in the visual cortex in response to salient internal states and environmental events (for a review see, Hurley et al., 2004). In line with this, increased activation in the visual cortex has been found during the perception and expectation of arousing emotional stimuli opposed to less arousing and/or neutral stimuli (Bradley et al., 2003; Ueda et al., 2003). To conclude, both the salience and visual subnetwork may be involved in the detection and subsequent processing of salient stimuli.

Compared to individuals carrying the L-allele[1] of 5-HTTLPR, individuals carrying the S-allele have demonstrated increased activation in brain regions implicated in salience and visual processing during fear learning, anticipation of aversive stimuli and emotion processing (Drabant et al., 2012; Herrmann et al., 2007; Klucken et al., 2013). These findings may be explained by attention biases in information processing, as studies have revealed that S-allele carriers have more difficulty in disengaging themselves from emotional stimuli (e.g. negative facial expressions) than L-allele carriers (Beevers et al., 2009; Koizumi et al., 2010; Pérez-Edgar et al., 2010; for a recent review, see Jonassen and Landro, 2014). Such biases have also consistently been found in depression and have been related to an over-responsive salience subnetwork (Hamilton et al., 2013). Thus, our finding of higher information processing efficiency in the salience and visual subnetwork may be related to more focused attention on threatening and negative emotional stimuli in the risk genotype group compared to the non-risk genotype group. This deserves further investigation in future research.

A potential explanation for heightened emotional reactivity in S-allele carriers, may be less efficient cognitive control of prefrontal regions (PFC) over limbic structures (Jonassen and Landro, 2014). In line with this proposition, studies have found both increased activation in PFC regions and reduced functional connectivity between the amygdala and PFC regions in S-allele carriers compared to L-allele carriers during emotion processing and executive functioning (Jonassen et al., 2012; Stollstorff et al., 2013; Surguladze et al., 2008; Volman et al., 2013). Furthermore, during reappraisal of negative emotional pictures, individuals homozygous for the S-allele showed no reductions in negative mood and increased activation of the superior frontal gyrus and anterior insula compared to individuals homozygous for the L-allele (Firk et al., 2013). These findings may indicate that S-allele carriers show less efficient and less effective top-down cognitive control over negative emotions compared to L-allele carriers. Accordingly, we found fewer connections between cognitive control subnetworks and other functional subnetworks in the risk genotype group compared to the non-risk genotype group in the current study. In conclusion, our findings may suggest that risk genotype carriers compared to non-risk genotype carriers have an increased tendency to appraise the environment as more threatening and are more sensitive to negative emotional stimuli, due to reduced cognitive control. This has also been proposed in a recent review of Jonassen and Landro (2014) as an underlying mechanism that may explain the behavioural disadvantage observed in S carriers, while they attempt to cognitively control negative emotions.

1 The studies discussed in the section '5-HTTLPR' of the discussion use different genotype group definitions: i) S homozygotes versus L carriers (Drabant et al., 2012; Klucken et al., 2013; Koizumi et al., 2010; Volman et al., 2013), ii) S carriers versus L homozygotes (Beevers et al., 2009; Herrmann et al., 2007), iii) S homozygotes versus L homozygotes (Beevers et al., 2009; Firk et al., 2013; Stollstorff et al., 2013), iv) S homozygotes versus heterozygotes versus L homozygotes (Jonassen et al., 2012; Pérez-Edgar et al., 2010; Surguladze et al., 2008). In sum, it varies per study whether the heterozygote group is included in the SS or LL group, is omitted or is an independent group. For this reason, we used the terms S carriers and L carriers, when describing the results of studies using different genotype group definitions. The exact genotype group definitions of each study can be found in this footnote.

8.5.2 COMT

For COMT, in the risk haplotype group compared to the non-risk haplotype group, we found a whole-brain functional network structure that resembles more that of a random network, that is, less functional segregation (Latora and Marchiori, 2001; Watts and Strogatz, 1998; Xia and He, 2011). Specifically, we observed that efficiency coefficients were lower in the DMS and that the FPS had fewer connections with other functional subnetworks. The finding related to the DMS is in line with prior research showing extensive decreases in DMS connectivity between mostly PFC regions and the posterior cingulate cortex (PCC) in Val homozygotes (COMT val158met) compared to heterozygotes (Liu et al., 2010), Met carriers (Tian et al., 2013) or only heterozygotes and not Met homozygotes (i.e. inverted U-shape) (Dang et al., 2012). Furthermore, the latter study found a relationship between lower DMS connectivity and slower responses during a set shifting task, which may suggest less efficient cognitive processing (Dang et al., 2012). The finding related to the FPS is in accordance with studies on COMT val^{158}met demonstrating less efficient cognitive processing in PFC regions that are part of the FPS in Val-allele carriers compared to Met-allele carriers (for a meta-analysis, see Mier et al., 2010).

8.5.3 COMT and neuroticism

For COMT, in the risk haplotype group (not in the non-risk haplotype group), we found that individuals scoring higher on neuroticism had a whole-brain functional network organization that resembles more that of a random network organization, i.e. increased functional integration and decreased functional segregation, compared to individuals scoring lower (Latora and Marchiori, 2001; Watts and Strogatz, 1998; Xia and He, 2011). Specifically, neuroticism was associated with i) lower efficiency coefficients for salience and sensory(-motor) subnetworks (COS, VS and SMS) and ii) more connections between the FPS and other functional subnetworks. Previous research has demonstrated a link between dopaminergic functioning and salience processing in healthy individuals as well as patients with schizophrenia and depression (Gradin et al., 2011; for a review on this topic in depression and schizophrenia, see Hamilton et al., 2012 and Winton-Brown et al., 2014, respectively). Increases in the neurotransmitter dopamine in mesolimbic, mesocortical and nigrostriatal sites have been shown in response to a wide range of arousing salient stimuli, such as strong aversive stimuli and sensory stimuli of high intensity and with a rapid onset (Horvitz, 2000). Therefore, it has been proposed that dopamine may be involved in the general detection of prediction errors (i.e. the discrepancy between expected and actual outcomes) and not only in reward prediction errors (for a review, see Horvitz, 2000). Particularly, the salience subnetwork was suggested to be involved in this process (Hauser et al., 2014; Winton-Brown et al., 2014). Furthermore, dopamine neurons in sensory(-motor) subnetworks have also been implicated in the detection and exploration of salient stimuli by modulating attention and triggering adaptive behavioural responses, respectively (Bromberg-Martin et al., 2010; Winton-Brown et al., 2014). Indeed, during emotional salience detection, a recent study has demonstrated that dopamine

modulated activation in brain regions involved in sensory processing, salience processing and emotion processing, such as the occipital cortex, amygdala, hippocampus, striatum, insula, and frontal/cingulate regions (Jabbi et al., 2013). Thus, in the current study, the finding of reduced information processing efficiency in salience and sensory(-motor) subnetworks may be related to impaired prediction and anticipation of salient events in high compared to low neurotic individuals in the risk haplotype group. This may hamper associative learning in these high neurotic individuals, thereby increasing feelings of uncertainty (for a review, see Palaniyappan and Liddle, 2012).

Furthermore, in the risk haplotype group (not in the non-risk haplotype group), we found that the FPS had relatively more connections with other functional subnetworks in high compared to low neurotic individuals. This finding may be interpreted as a compensatory mechanism, i.e. increased cognitive control, in response to the observed reduction in information processing efficiency in the salience and sensory(-motor) subnetworks in these high neurotic individuals (Doucet et al., 2011; Laird et al., 2011). Aforementioned interpretations are in line with our model of emotion processing in neuroticism (Servaas et al., 2013b), wherein we proposed that a more active fear learning system may lead to difficulties in the anticipation of aversive stimuli, requiring increased cognitive control. Accordingly, in depression, evidence has been found for the hypothesis of reduced dopamine function - leading to dysfunctional salience processing and error prediction - being associated with feelings of anhedonia (Gradin et al., 2011). In addition, COMT variation has also been implied in depression, although not robustly (Opmeer et al., 2010).

8.5.4 Limitations

Several limitations of this study need to be considered. First, we had no direct measures of serotonin and dopamine levels in the different functional subnetworks. Second, although our sample size is relatively large, it was too small to investigate interactions between the two polymorphisms 5-HTTLPR and COMT. Third, we tested associations between 5-HTTLPR/COMT, functional brain network organization and neuroticism. For future research, it would be of interest to determine the causal relations between these factors, to investigate the validity of models proposed by the endophenotype approach (e.g. mediational model) (Kendler and Neale, 2010). Does polymorphic-dependent neurotransmission indeed influence neural (network) plasticity (in interaction with the (early) environment) that causes neuroticism (Hahn et al., 2011, 2013)? Though interesting, it is challenging to investigate, since i) functioning of neurotransmission is extremely complex, ii) causal effects are difficult to determine, iii) there are other unknown factors at work (e.g. pleiotropy, epistasis and gene-by-environment interactions) and iv) pathways have small effect sizes (Canli, 2008; Hahn et al., 2011, 2013). More in vitro (e.g. gene expression quantification), in vivo (e.g. single photon emission computed tomography, SPECT) and longitudinal studies are necessary. Fourth, we only investigated female students and therefore, our findings cannot be generalized to the whole population. Future studies should replicate our results

in, for example, male samples. However, by selecting a homogenous sample, we controlled for several important confounders, such as gender, age, education level and ethnicity. Fifth, we used a univariate approach in the current study. It is known that univariate analyses do not capture the full complexity of brain networks (Simpson et al., 2013). Multivariate approaches are currently being developed to investigate the effects of multiple measures on the network organization (Simpson et al., 2013). For this reason, our results should be considered exploratory and further validation is needed.

8.6 Conclusion

The aim of the current study was to investigate the triadic interplay between 5-HTTLPR/COMT, functional brain network organization and neuroticism. For both polymorphisms, we found an altered functional network organization in genetic risk carriers compared to non-risk carriers. Specifically, the findings showed that subnetworks related to salience and visual processing play a more prominent role in the functional network organization of genetic risk carriers, than subnetworks related to cognitive control. This may generate the hypothesis that genetic risk carriers compared to non-risk carriers perceive the world as more threatening and express heighted emotional reactivity to negative events, possibly due to reduced cognitive control. For COMT, in the risk haplotype group (not the non-risk haplotype group), neuroticism was associated with i) lower efficiency coefficients for salience and sensory(-motor) subnetworks and ii) relatively more connections between the fronto-parietal control subnetwork and other functional subnetworks. In the risk haplotype group, these findings may indicate that high compared to low neurotic individuals show impairments in the prediction and anticipation of salient events, requiring increased cognitive control to process the sensory overload. In conclusion, our findings of altered topology of specific subnetworks may help explain why risk carriers of the 5-HTTLPR and COMT (scoring higher on neuroticism) have difficulties in emotion processing and are more prone to develop psychopathology. The current study illustrates the added value of using connectomic measures in genetic imaging. Future studies may use this method to further investigate the relationship between genetics and the functional network organization in healthy individuals as well as psychiatric patients.

8.7 Acknowledgements

The current study was supported by the Ministry of Education, Culture and Science of the Netherlands (609022). The sponsor did not play a role in the study design; collection, analysis and interpretation of the data; writing the report or the decision to submit the article for publication. In addition, the authors would like thank A. Sibeijn-Kuiper and J. Streurman-Werdekker for their support in the data acquisition and A.M. Brugman for DNA extraction and genotyping.

8.8 Supplementary material

8.8.1 S1 Overview of the full fMRI session

The full fMRI session consisted of four tasks, resting state and an anatomical scan. The following tasks/scans were presented in consecutive order: emotional face matching task (Hariri et al., 2002), mood (worry) induction paradigm (Paulesu et al., 2010), anatomical scan, resting state, interoceptive sensitivity task (Pollatos et al., 2007) and Ultimatum Game (Sanfey et al., 2003). The total duration of the fMRI session was approximately 60 minutes. The order was fixed and identical for all participants.

8.8.2 S2 Preprocessing steps

First, structural as well as functional images were reoriented parallel to the AC-PC plane. Second, functional images were realigned to the first image using rigid body transformations and the mean EPI image, created during this step, was coregistered to the anatomical T1 image. Third, structural images were corrected for bias field inhomogeneities, registered using linear transformations and segmented into grey matter (GM), white matter (WM) and cerebrospinal fluid (CSF) (MNI template space). Fourth, we used DARTEL (diffeomorphic anatomical registration through exponentiated lie algebra toolbox) (Ashburner, 2007) to create a customized group template to increase the accuracy of inter-subject alignment. Individual GM and WM tissue segments were iteratively aligned to the group template in order to acquire individual deformation flow fields. Fifth, the coregistered functional images were normalized to MNI space using the customized group template and individual deformation flow fields. Furthermore, images were resampled to 2 mm^3 isotropic voxels and smoothed with a 8 mm full-width at half-maximum (FWHM) Gaussian kernel.

8.8.3 S3 Scrubbing procedure: framewise displacement and DVARS

The indices framewise displacement (FD) and DVARS were calculated to indicate volumes (i.e. frames) that may be affected by motion artifacts (Power et al., 2012). FD is calculated as the root of the sum of the squared differentials per volume. Rotations were converted to translations assuming a distance of 65 mm from the origin of rotation (ArtRepair toolbox, http://cibsr.stanford.edu/tools/human-brain-project/artrepair-software.html). DVARS is calculated as the root mean square (RMS) of the derivatives of the time series across voxels included in the whole-brain mask per volume (Power et al., 2011, 2012). Volumes were removed when FD>0.5 mm and DVARS>mean + 3*SD. Additionally, one backward and two forward neighboring volumes were removed as well. The median of the number of scans that were removed per subject was 11.0 (IQR = 14.2). Subjects were excluded when more than one third of the volumes had to be removed. After scrubbing, neuroticism scores did not correlate with mean head displacement, maximum head displacement,

head rotation and the number of micromovements (<0.1 mm) (p>0.17) (van Dijk et al., 2010). Furthermore, neuroticism did not correlate with the number of removed scans (p = 0.63).

8.8.4 S4 Module decomposition

A two-step procedure was applied to achieve the optimal modular structure using a threshold of 1.8% (see S5 for details on the selection of this threshold). Input for this procedure was the binarized correlation matrix averaged across subjects. First, nodes were partitioned into modules using the algorithm of Blondel et al. (2008), wherein nodes are divided in groups with a maximum number of within-group edges and a minimum number of between-group edges. This calculation was repeated 500 times to increase the chance of escaping local maxima. The statistic was further optimized by applying the modularity fine-tuning algorithm of Sun et al. (2009), wherein nodes are randomly assigned to other modules until modularity no further improves.

8.8.5 S5 Selection of an optimal threshold for module decomposition

First, correlation matrices were binarized using a range of threshold values (T=0.01-0.30 in increments of 0.01). Second, these matrices were averaged across subjects per threshold value and the entropy was calculated for each of them to indicate for which threshold value the edges showed the largest stability information-wise (lowest entropy). These results were compared to results obtained via randomized matrices (for details, see Geerligs et al., 2014). The optimal threshold is the threshold where (i) the original matrix shows the largest stability across subjects (low entropy) and (ii) the difference in entropy is the largest between the original matrix and random matrix. The optimal threshold in the current study was 1.8%.

8.8.6 S6 Correlation values for the relationship between the network measures and neuroticism per genetic group

Table S1 Correlation values for the relationship between the network measures and neuroticism per genetic group

	Proportional threshold in %																													
	1	**2**	**3**	**4**	**5**	**6**	**7**	**8**	**9**	**10**	**11**	**12**	**13**	**14**	**15**	**16**	**17**	**18**	**19**	**20**	**21**	**22**	**23**	**24**	**25**	**26**	**27**	**28**	**29**	**30**
COMT Binary, Global efficiency, Whole-brain																														
Risk r	.23	.25	.29	.30	.33	.36	.37	.40	.42	.44	.46	.47	.47	.48	.47	.47	.46	.46	.47	.46	.47	.47	.48	.48	.48	.48	.48	.47	.47	.46
Non-risk r	.00	.07	.06	.07	.10	.11	.11	.13	.14	.13	.12	.11	.11	.12	.12	.12	.14	.13	.13	.14	.14	.13	.13	.13	.13	.13	.13	.13	.12	.12
COMT Binary, Local efficiency, VS																														
Risk r	-.27	-.22	-.18	-.23	-.32	-.38	-.38	-.38	-.39	-.39	-.39	-.39	-.38	-.42	-.45	-.44	-.45	-.44	-.45	-.46	-.46	-.46	-.46	-.47	-.47	-.46	-.46	-.46	-.46	-.46
Non-risk r	.00	.03	.04	.08	.04	.04	.03	-.01	-.03	-.03	-.05	-.07	-.10	-.11	-.15	-.16	-.17	-.20	-.20	-.20	-.19	-.20	-.19	-.19	-.19	-.19	-.20	-.19	-.19	-.19
COMT Binary, Participation coefficient, FPS																														
Risk r	.26	.25	.29	.28	.20	.19	.23	.26	.25	.26	.26	.29	.30	.32	.32	.33	.32	.32	.31	.32	.32	.33	.33	.32	.33	.33	.33.	33	.32	.33
Non-risk r	-.07	-.05	-.09	-.06	-.07	.01	.01	.03	.05	.03	.06	.08	.12	.12	.09	.10	.10	.09	.09	.10	.10	.11	.10	.10	.10	.10	.09	.09	.10	.10
COMT Weighted, Local efficiency, Whole-brain																														
Risk r	-.06	-.10	-.22	-.29	-.39	-.41	-.41	-.43	-.46	-.47	-.46	-.46	-.47	-.47	-.47	-.47	-.47	-.47	-.47	-.47	-.47	-.47	-.47	-.47	-.47	-.47	-.47	-.47	-.47	-.47
Non-risk r	-.06	-.04	-.02	.03	.04	-.01	-.06	-.06	-.06	-.06	-.06	-.08	-.09	-.10	-.10	-.10	-.11	-.11	-.11	-.11	-.11	-.11	-.11	-.12	-.11	-.12	-.12	-.12	-.12	-.12

Table S1 Continued

	Proportional threshold in %																													
	1	**2**	**3**	**4**	**5**	**6**	**7**	**8**	**9**	**10**	**11**	**12**	**13**	**14**	**15**	**16**	**17**	**18**	**19**	**20**	**21**	**22**	**23**	**24**	**25**	**26**	**27**	**28**	**29**	**30**
COMT Weighted, Local efficiency, COS																														
Risk r	.19	.18	.15	.11	.04	.00	-.03	-.13	-.19	-.27	-.32	-.37	-.41	-.41	-.42	-.45	-.45	-.45	-.44	-.44	-.44	-.43	-.43	-.42	-.42	-.42	-.42	-.42	-.41	-.41
Non-risk r	.08	.13	.07	.16	.18	.13	.07	.08	.10	.07	.09	.05	.02	-.01	-.02	-.03	-.02	-.03	-.02	-.02	-.01	-.01	-.01	-.01	-.01	.00	.00	.00	.01	.00
COMT Weighted, Local efficiency, SMS																														
Risk r	-.15	-.24	-.33	-.36	-.47	-.44	-.46	-.46	-.47	-.47	-.49	-.48	-.49	-.50	-.49	-.49	-.50	-.50	-.50	-.50	-.50	-.50	-.50	-.50	-.50	-.50	-.50	-.50	-.50	-.50
Non-risk r	-.11	-.13	-.05	-.01	-.01	-.04	-.13	-.12	-.11	-.13	-.15	-.15	-.14	-.14	-.12	-.13	-.13	-.13	-.13	-.14	-.14	-.14	-.15	-.15	-.15	-.14	-.15	-.15	-.15	-.15
COMT Weighted, Local efficiency, VS																														
Risk r	-.31	-.29	-.28	-.32	-.39	-.43	-.44	-.44	-.45	-.46	-.46	-.46	-.45	-.47	-.47	-.47	-.47	-.47	-.47	-.47	-.47	-.47	-.47	-.47	-.47	-.47	-.47	-.47	-.47	-.47
Non-risk r	-.01	.01	.02	.04	.02	.00	-.01	-.02	-.03	-.03	-.03	-.04	-.05	-.05	-.07	-.08	-.08	-.09	-.09	-.09	-.09	-.09	-.09	-.10	-.10	-.10	-.11	-.11	-.11	-.11

The correlation values are given for each proportional threshold value. COMT, catechol-O-methyltransferase; COS, cingulo-operculum subnetwork; FPS, fronto-parietal subnetwork; SMS, somatosensory-motor subnetwork; VS, visual subnetwork.